

# Frictional Energy Dissipation in a Contact of Elastic Bodies Subjected to Superimposed Normal and Tangential Oscillations

T. Hanisch<sup>1</sup>, I. Richter<sup>1</sup>, and Q. Li<sup>1\*</sup>

<sup>1</sup> *Technische Universität Berlin, Berlin, 10623 Germany*

\* *e-mail: qiang.li@tu-berlin.de*

Received March 16, 2020, revised March 16, 2020, accepted March 24, 2020

**Abstract**—Frictional damping in elastic contact of a parabolic indenter subjected to a combination of oscillations in normal and tangential directions is numerically simulated. The dissipated energy first increases linearly with coefficient of friction, then decreases linearly, and finally reaches a constant value. These three regions correspond to the states of complete slip, partial slip and complete stick. All three asymptotical dependencies can be described analytically. The dissipated energy in a dimensionless form is function of the ratio of normal oscillation amplitude and mean indentation depth, the ratio of change in contact area and sticking area, and phase shift between normal and tangential oscillation. Master curves are suggested.

*Keywords:* friction, energy dissipation, stick-slip, dual oscillation, elastic contact, contact mechanics

**DOI:** 10.1134/S1029959920060119

## 1. INTRODUCTION

In frictional contacts, energy is dissipated when two contacting bodies have a relative sliding movement. For elastic bodies, it is well known that under the periodic oscillating loading in tangential direction, the microslip appears at the boundary of contact and stick in the middle of contact, which may lead to fretting and initiation of fatigue cracks [1]. This frictional damping occurs very common in the interface of joints of machine components [2, 3] and plays an important role in many applications of tribology and structure mechanics [4]. The energy dissipation of a spherical indenter subject to tangential oscillation was analyzed early by Mindlin [5]. It was found that the dissipated energy in one cycle is inversely proportional to the coefficient of friction, which indicates that there will be no energy dissipation if the coefficient of friction is infinitely large, because the whole contact is in a state of stick. However, a recent study shows that even in the case of infinitely large coefficient, energy dissipation still occurs if the body oscillates in both vertical and tangential directions, because the elastic energy stored at the boundary elements of contact is suddenly relaxed during the composed oscillating process [6]. This kind of energy dissipation is called “relaxation damping”. In this paper, we numerical-

ly study the frictional damping due to a combination of vertical and tangential oscillation with constant coefficient of friction in contact under the Coulomb’s law of friction.

The energy dissipation under varying normal and tangential loading has been studied by many researchers, for example analytically by Davies et al. [7] for smooth two-dimensional indenters and by Putignano et al. [8] for rough surfaces, numerically by Liu and Eriten for two-dimensional wavy surfaces using the finite element method [9], and experimentally early by Johnson [10], Goodman and Brown [11] and recently by Usta et al. [12], where a power-law relation between dissipated energy and maximal applied stress has been intensively discussed and the power-law exponent is argued between 2 and 3. Furthermore, studies have shown that phase shift between normal and tangential oscillation plays an essential role in frictional energy dissipation [13, 14], and the maximal energy dissipation occurs in many cases when phase different is  $\pi/2$  [8, 14]. In this paper, we carry out simulations of contact due to a combination of normal and tangential oscillation using the method of dimensionality reduction [15–17]. This is a very effective analytical and numerical tool exactly for this type of contact problems where only the total macroscopic force and

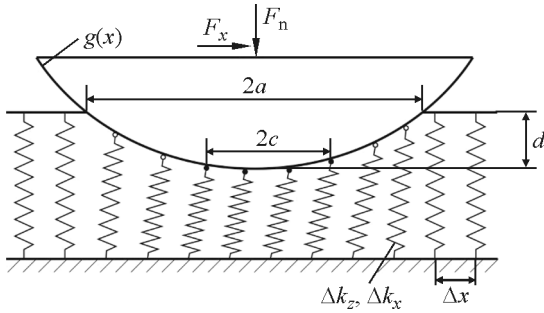


**Fig. 1.** Equivalent contact between a parabolic indenter and an elastic half space in the framework of the method of dimensionality reduction.

displacement are of importance. Both these quantities are determined in the framework of method of dimensionality reduction exactly, provided Coulomb's law of friction is assumed.

## 2. MATHEMATICAL MODEL

We consider a contact between a rigid parabolic indenter with profile  $f(r) = r^2/(2R)$  and an elastic half space with elastic modulus  $E$  and Poisson's ratio  $\nu$ , where  $R$  is radius of indenter and  $r$  polar radius in the contact plane. After indentation by  $d_0$ , indenter is forced to oscillate in vertical and tangential directions with angular frequency  $\omega$ , phase difference  $\varphi$  and small amplitudes  $\Delta u_z$  and  $\Delta u_x$  according to the following displacement-controlled laws:

$$\begin{aligned} u_z^{(0)}(t) &= d_0 + \Delta u_z^{(0)} \cos(\omega t), \\ u_x^{(0)}(t) &= \Delta u_x^{(0)} \cos(\omega t + \varphi). \end{aligned} \quad (1)$$

We consider the case of "no jumping" and small amplitude, therefore  $\Delta u_z \ll d_0$ .

In the framework of the method of dimensionality reduction, the three-dimensional profile is transformed into a plane profile according to [15, 16]

$$g(x) = |x| \int_0^{|x|} \frac{f'(r)}{\sqrt{x^2 - r^2}} dr. \quad (2)$$

For the parabolic indenter, its corresponding one-dimensional profile is given by  $g(x) = x^2/R$ . Furthermore, the elastic half space is replaced by a one-dimensional elastic foundation consisting of an array of independent springs with discrete distance  $\Delta x$  (Fig. 1). The normal and tangential stiffness of springs,  $\Delta k_z$  and  $\Delta k_x$  are defined following the rules:

$$\Delta k_z = E^* \Delta x, \quad \Delta k_x = G^* \Delta x, \quad (3)$$

where effective elastic modulus is  $E^* = E/(1 - \nu^2)$  and shear modulus  $G^* = 4G/(2 - \nu)$ . With profile and elastic foundation defined in Eqs. (2) and (3), one can

simply solve the normal or tangential contact problems. The normal and tangential forces on each spring in contact is easily calculated by its stiffness  $\Delta k_z$ ,  $\Delta k_x$  and displacement  $u_z(x, t)$  and  $u_x(x, t)$

$$\Delta f_z(x, t) = \Delta k_z u_z(x, t), \quad \Delta f_x(x, t) = \Delta k_x u_x(x, t). \quad (4)$$

The normal displacement is dependent of only the profile  $g(x)$  and the given normal oscillation  $u_z^{(0)}(t)$

$$u_z(x, t) = u_z^{(0)}(t) - g(x). \quad (5)$$

The tangential displacement can be determined by the following Coulomb's law of friction: firstly, we assume that all springs in contact are in stick state and have the same incremental tangential displacement as indenter. If the resulted tangential force on some spring is larger than the production of coefficient of friction  $\mu$  and normal force  $\Delta f_z(x, t)$ , then it is in a state of slip, and the tangential force should be corrected according to Coulomb's law. So, for a given small incremental displacement of indenter  $du_x^{(0)}(t)$ , we have the following rules

$$du_x(x, t) = du_x^{(0)}(t), \quad u_x(x, t) = \pm \frac{\mu \Delta f_z(x, t)}{\Delta k_x}. \quad (6)$$

The details on application of the method of dimensionality reduction to normal and tangential contact can be found in paper [15]. With obtained tangential displacement of springs one can then calculate the force according to Eq. (4) as well as the total tangential force by summing the spring forces

$$F_x(t) = \sum_{\text{cont}} \Delta f_x(x, t).$$

The energy in one period of oscillation  $T = 2\pi/\omega$  is then given as

$$W = \int_0^T F_x(t) du_x^{(0)}(t). \quad (7)$$

## 3. RESULTS

### 3.1. Theoretical Analysis

Before presenting numerical results, we introduce the existing important results from the literature and offer a brief discussion on the current study. In the case of only tangential oscillation with finite coefficient of friction, the dissipated energy in one period of oscillation was given by Mindlin [5, 15]

$$W_M = \frac{2}{3} \kappa^{-2} E^* R^{1/2} d_0^{-1/2} (\Delta u_x^{(0)})^3 \mu^{-1}, \quad (8)$$

where  $\kappa = E^*/G^*$ . It is inversely linear function of coefficient of friction, thus there will be no energy dissipation if coefficient of friction is infinitely large  $\mu = \infty$ . However, in the case of composition of vertical and

tangential oscillation according to Eq. (1), the relaxation damping with  $\mu = \infty$  appears and it was given by Popov et al. [6]

$$W_\infty = \frac{8}{3} G^* R^{1/2} d_0^{-1/2} \Delta u_z^{(0)} (\Delta u_x^{(0)})^2 \sin^2 \varphi. \quad (9)$$

The maximal damping  $W_{\infty, \max}$  occurs when the phase shift is  $\varphi = \pi/2$ :

$$W_{\infty, \max} = \frac{8}{3} G^* R^{1/2} d_0^{-1/2} \Delta u_z^{(0)} (\Delta u_x^{(0)})^2. \quad (10)$$

Considering another limiting case of very small coefficient of friction where the whole contact area is in a state of slip, then the tangential force is simply following the Coulomb's law of friction:  $F_x = \mu F_n$ , and the dissipated energy in one oscillation cycle is equal to

$$W_C = \mu F_n 4 \Delta u_x^{(0)}. \quad (11)$$

Substitution of solution of normal load in Hertzian contact,  $F_n = 4/3 E^* R^{1/2} d_0^{3/2}$  (we assume  $\Delta u_z \ll d_0$ , so the influence of vertical amplitude is neglected) into Eq. (11) provides

$$W_C = 16/3 \mu E^* R^{1/2} d_0^{3/2} \Delta u_x^{(0)}. \quad (12)$$

Equations (8), (9), (12) are three analytical solutions which will be used in the following analysis.

Now we discuss one important parameter in description of energy dissipation: the ratio of the change in contact area and sticking area  $\Delta a/\Delta c$ . For the normal contact, it is well known that the contact radius is geometrically related to indentation depth  $d$  and sphere radius  $a = \sqrt{Rd}$ , so derivative of contact radius with respect to indentation depth results in the change in contact radius

$$\Delta a = \frac{1}{2} \sqrt{\frac{R}{d}} \Delta d. \quad (13)$$

In an oscillating contact, the maximum change in indentation depth is  $\Delta d = 2 \Delta u_z^{(0)}$ , then Eq. (13) becomes

$$\Delta a = R^{1/2} d^{-1/2} \Delta u_z^{(0)}. \quad (14)$$

For tangential contact, the contact radius of sticking area  $c$  is determined by the relation (the normal amplitude of oscillation is still neglected compared with mean indentation depth)

$$G^* u_x^{(0)} = \mu E^* (d_0 - g(c)) = \mu E^* \left( d_0 - \frac{c^2}{R} \right). \quad (15)$$

Similar to normal oscillation, considering the maximal change in tangential displacement (absolute value), it has,

$$|2 \Delta u_x^{(0)}| = |\mu \kappa R^{-1} \cdot 2c \Delta c|. \quad (16)$$

For small amplitude of oscillation, the radius of slip area is also very small, then we have  $c \approx a = \sqrt{Rd}$  in comparison with  $\Delta c$ . Following that Eq. (16) has the form

$$\Delta c = \Delta u_x^{(0)} R^{1/2} d^{-1/2} \mu^{-1} \kappa^{-1}. \quad (17)$$

From Eqs. (14) and (17) the ratio of change in contact area and sticking area  $\Delta a/\Delta c$  is then equal to

$$\bar{\mu} = \frac{\Delta a}{\Delta c} = \frac{\Delta u_z^{(0)}}{\Delta u_x^{(0)}} \mu \kappa, \quad (18)$$

which is denoted by  $\bar{\mu}$ .

In this study, we consider dual oscillation but with finite coefficient of friction, the numerically obtained dissipated energy will be normalized by the maximal value  $W_{\infty, \max}$  in the limiting case of  $\mu = \infty$  in Eq. (9) with  $\varphi = \pi/2$ . Then the normalized solution by Mindlin in Eq. (8) is

$$\frac{W_M}{W_{\infty, \max}} = \frac{1}{4} \left( \frac{\Delta u_z^{(0)}}{\Delta u_x^{(0)}} \mu \kappa \right)^{-1}, \text{ or } \bar{W}_M = \frac{1}{4 \bar{\mu}}. \quad (19)$$

The solution for the case of complete slip (12) in the normalized form is

$$\frac{W_C}{W_{\infty, \max}} = 2 \left( \frac{d_0}{\Delta u_z^{(0)}} \right)^2 \frac{\Delta u_z^{(0)}}{\Delta u_x^{(0)}} \mu \kappa, \text{ or } \bar{W}_C = 2 \bar{\delta}^{-2} \bar{\mu} \quad (20)$$

with ratio of normal oscillation amplitude and mean indentation depth

$$\bar{\delta} = \frac{\Delta u_z^{(0)}}{d_0}. \quad (21)$$

Normalized solution for relaxation damping (9) is then phase dependent

$$\bar{W}_\infty = \frac{W_\infty}{W_{\infty, \max}} = \sin^2 \varphi. \quad (22)$$

From Eqs. (19), (20) and (22), we can see that the normalized dissipated energy in case of Mindlin depends only on  $\bar{\mu}$ , in the case of relaxation damping by Popov et al. only on phase  $\varphi$ , and in the case of Coulomb on both  $\bar{\delta}$  and  $\bar{\mu}$ . In the following part, numerical results show that the dimensionless energy dissipation in one oscillation period in a general case is a function of these three parameters:

$$\bar{W} \sim f(\bar{\delta}, \bar{\mu}, \varphi). \quad (23)$$

### 3.2. Numerical Results

The frictional contact was numerically simulated using the method of dimensionality reduction as de-

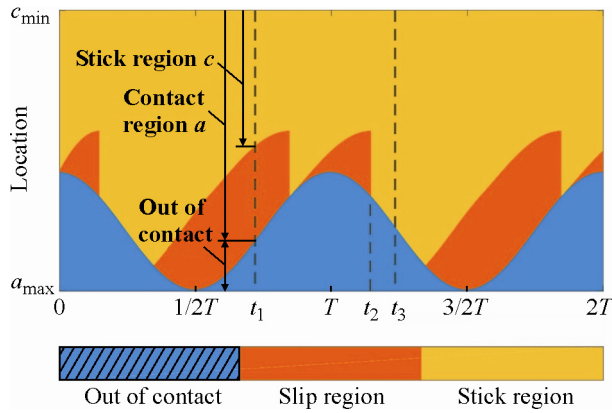


**Fig. 2.** Map of slip, stick, and noncontact area in two cycles of oscillation for parameter set:  $\varphi = \pi/2$ ,  $\bar{\mu} = 0.7268$  and  $\bar{\delta} = 0.01$  (color online).

scribed in Sect. 2. Figure 2 shows an example of contact area, sticking area and area out of contact changing with time in two cycles of oscillation  $2T$  for parameter  $\varphi = \pi/2$ ,  $\bar{\mu} = 0.7268$  and  $\bar{\delta} = 0.01$ . Vertical axis shows the coordinate in plane ranging from the minimal boundary of stick-slip area  $c_{min}$  to the maximal contact radius  $a_{max}$ . One can see that the contact radius varies with a harmonic-like function which could be also analytically calculated according to  $a(t) = (Ru_z^{(0)}(t))^{1/2}$ . Focus on only one time moment, for example at time  $t_1$  (dashed line in Fig. 2), there is a stick region in the middle (upper part in yellow), slip region at the contact boundary (middle part in orange), and noncontact region (lower part in blue). But from the map it is seen that slip does not exist all the time, for example at time  $t_3$  the whole contact is in a state of sticking. Thus, energy dissipation occurs not all the time, but only in the time intervals when slip appears. Interestingly, one can see that in dual oscillation, the

slip region appears and spreads gradually, but vanishes suddenly to a state of complete stick (for example at time  $t_2$ ).

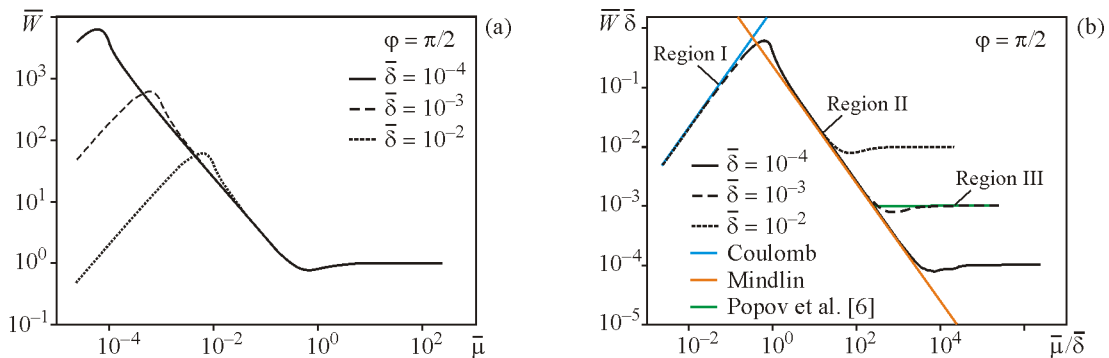
A phenomenon should be noted here: in Fig. 2 the first cycle behaves slightly differently than the following one. The reason for that is the initiation of spring locations, therefore only the second cycle is considered below for the calculation of the dissipated energy per cycle.

Figure 3a shows the dependence of the normalized dissipated energy  $\bar{W}$  on the parameter  $\bar{\mu}$  for phase  $\varphi = \pi/2$  and three different values of  $\bar{\delta} = 10^{-4}$ ,  $10^{-3}$  and  $10^{-2}$ . The parameter  $\bar{\mu}$  was changed by varying the coefficient of friction  $\mu$ . Focus on one single curve, one can see that the dissipated energy increases with coefficient of friction as well as parameter  $\bar{\mu}$ , then it decreases until reaches to a constant value.

This dependence can be divided into three regions:

- a linear dependence in region I where the complete slip occurs according to Coulomb’s law of friction described by Eq. (20),
- an inversely proportional dependence in region II which can be described by the Mindlin’s solution (Eq. (19)) for a state of partial sliding, and
- constant value in the region III corresponding to the pure “relaxation damping” for a state of complete sticking described by Popov et al. in Eq. (22) [6].

In this normalized form, three curves overlap at large value of  $\bar{\mu}$  in regions II and III where the energy is independent of  $\bar{\delta}$ , and the normalized dissipated energy is equal to 1 in the plateau with this example  $\varphi = \pi/2$ :  $\bar{W} = 1$ . A multiplication of the normalized dissipated energy by the ratio  $\bar{\delta}$  and its reciprocal by  $\bar{\mu}$ , as shown in Fig. 3b, leads to an overlap of the curves at small ratios of  $\bar{\mu}/\bar{\delta}$  in regions I and II. These behaviors can be described by Eqs. (19)–(22).



**Fig. 3.** Dependence of dissipated energy on parameter  $\bar{\mu}$  for different amplitudes of normal oscillation  $\bar{\delta}$  from  $10^{-4}$  to  $10^{-2}$ : the curves overlap at large values of  $\bar{\mu}$  (a); the curves overlap at small values of  $\bar{\mu}/\bar{\delta}$  (b) if the coordinates are multiplied by  $\bar{\delta}$  and its reciprocal (color online).

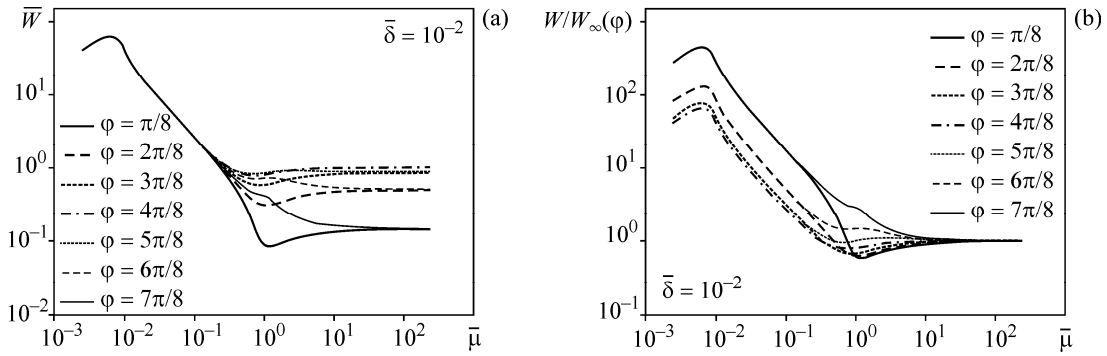


**Fig. 4.** Dependence of dissipated energy on parameter  $\bar{\mu}$  for different phases for  $\bar{\delta} = 10^{-2}$ . The energy is normalized by  $W_{\infty, \max}$  (a) and by  $W_{\infty}(\varphi)$  (b) in its corresponding phase  $\varphi$ .

In Fig. 4a the dependences of dissipated energy  $\bar{W}$  on parameter  $\bar{\mu}$  for  $\bar{\delta} = 10^{-2}$  and different phases  $\varphi$  are shown. A master curve is generated at small values of  $\bar{\mu}$  in regions I and II, so the dissipated energy is independent of phase in this range. With increasing coefficient of friction, they are dispersed because the dissipated energy with very large coefficient of friction in the case of relaxation damping is phase dependent. If the energy is normalized as  $W/W_{\infty}(\varphi)$  by taking into account the phase angle, then the curves tends towards  $W/W_{\infty}(\varphi) = 1$  in the region of plateau (Fig. 4b).

To find an “empirical” equation describing all three regions, two options are presented below.

The first possibility is to describe three regions separately with already known theories, as discussed above:

$$\left\{ \begin{array}{l} \bar{W} = 2 \frac{\bar{\mu}}{\bar{\delta}^2}, \text{ region I, for } 0 \leq \bar{\mu} \leq \frac{1}{\sqrt{8}} \bar{\delta}, \\ \bar{W} = \frac{1}{4\bar{\mu}}, \text{ region II, for } \frac{1}{\sqrt{8}} \bar{\delta} \leq \bar{\mu} \leq \frac{1}{4\sin^2 \varphi}, \\ \bar{W} = \sin^2 \varphi, \text{ region III, for } \bar{\mu} \geq \frac{1}{4\sin^2 \varphi}. \end{array} \right. \quad (24)$$

The boundary between two regions are simply obtained by equilibrium of two equations. These three relations are shown in Fig. 3b with solid lines. In Figs. 3 and 4 numerical results show that there is a smooth transition between regions I and II, as well as between regions II and III. However, Eq. (24) does not cover these transition zones.

Another possibility is to approximate the simulation results using rational functions. For region I, beginning of region II and their transition, a perfect master curve is observed as seen in Figs. 3b and 4a, the results are dependent of  $\bar{\delta}$  but independent of phase

$\varphi$ . Taking  $\bar{\delta}$  into account, we have the following rational function for  $0 \leq \xi_1 \leq 4$ :

$$\begin{aligned} \bar{W}\bar{\delta} = & (4.858 \cdot 10^{-4} \xi_1^5 + 0.2203 \xi_1^4 - 0.2226 \xi_1^3 \\ & - 0.1252 \xi_1^2 + 0.1836 \xi_1)(\xi_1^5 - 1.932 \xi_1^4 + 1.482 \xi_1^3 \\ & - 0.5866 \xi_1^2 + 0.0779 \xi_1 + 0.0889)^{-1} \end{aligned} \quad (25)$$

with definition of parameter

$$\xi_1 = \frac{\bar{\mu}}{\bar{\delta}}. \quad (26)$$

This approximation is shown in Fig. 5 on the left side with the example of  $\bar{\delta} = 10^{-2}$ , which agrees with numerical results very well. It is noted that the range of  $\xi_1$  in Eq. (25) is evaluated based on the curves in Fig. 3b. For other cases, for example  $\bar{\delta} > 10^{-2}$ , the range will be reduced. The importance of (25) is the description of transition zone, so for the linear part, more exact solution (24) is suggested.

For the other transition between regions II and III, one can see that shape of the curves in this area are different for different phases  $\varphi$  (Fig. 4), thus a master curve cannot be generated, therefore we give here only an approximation for a special case of  $\varphi = \pi/2$  for  $\bar{\mu} \geq 10^{-1}$ :

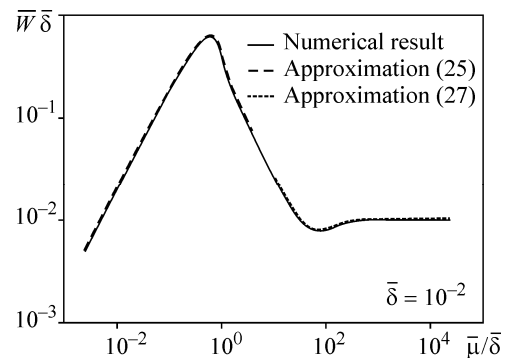


**Fig. 5.** Approximation to the numerical result using rational functions.

$$\begin{aligned} \bar{W} = & (\bar{\mu}^4 + 0.7169\bar{\mu}^3 + 0.2668\bar{\mu}^2 + 0.3342\bar{\mu} \\ & - 40017 \cdot 10^{-6})(\bar{\mu}^4 + 0.5979\bar{\mu}^3 \\ & + 1.335\bar{\mu}^2 - 5.079 \cdot 10^{-5}\bar{\mu})^{-1}. \end{aligned} \quad (27)$$

#### 4. CONCLUSION

The frictional contact of a parabolic indenter and an elastic half space, while the indenter is subjected to oscillations in normal and tangential directions, is numerically simulated using the method of dimensionality reduction. The dissipated energy in one oscillation cycle is studied for different coefficients of friction, oscillation amplitudes and phase shifts between vertical and horizontal direction. It is found that the dissipated energy increases linearly with coefficient of friction (region I), then decreases linearly (region II), finally reaches to constant (region III). These three regions correspond to states of complete slip, partial slip and complete stick. The can be described by the known asymptotic solutions based on the Coulomb's law of friction, Mindlin's solution and solution for relaxation damping.

The dissipated energy in dimensionless form occurs to be function of only three dimensionless parameters: normal oscillation amplitude, ratio of change in contact radius and radius of sticking area, and phase shift. Depending on these parameters, two master curves were obtained covering the most part of region, but not the transition between regions II and III where the shape of curves is phase dependent. The dependences in these three regions can be described very well by use of existing analytical solutions, and transitions between them can be defined roughly by their intersection points. The second possibility of approximations is to specify the curve by two rational functions. With that a fairly precise calculation was applies to the case of phase shifts of  $\pi/2$ . For other phase shifts or very large ratios of vertical vibration amplitude to depth of indentation, the numerical simulation should be used as the calculation method.

#### ACKNOWLEDGMENTS

The authors would like to thank V.L. Popov for his advice and contributions to develop the theoretical modelling.

#### REFERENCES

1. Popov, V.L., *Contact Mechanics and Friction*, Springer, 2017.
2. Ahn, Y.J., Relaxation Damping and Friction, *Int. J. Mech. Sci.*, 2017, vol. 128–129, pp. 147–149.
3. Peyret, N., Dion, J.L., Chevallier, G., and Argoul, P., Micro-Slip Induced Damping in Planar Contact under Constant and Uniform Normal Stress, *Int. J. Appl. Mech.*, 2010, vol. 2(2), pp. 281–304.
4. Gagnon, L., Morandini, M., and Ghiringhelli, G.L., A Review of Friction Damping Modeling and Testing, *Arch. Appl. Mech.*, 2020, vol. 90, pp. 107–126.
5. Mindlin, R.D., Mason, W.P., Osmer, J.F., and Dere-siewicz, H., Effects of an Oscillation Tangential Force on the Contact Surfaces of Elastic Spheres, in *Proceedings of 1st US National Congress of Applied Mechanics*, 1952, pp. 203–208.
6. Popov, M., Popov, V.L., and Pohrt, R., Relaxation Damping in Oscillating Contacts, *Sci. Rep.*, 2015, vol. 5, p. 16189.
7. Davies, M., Barber, J.R., and Hills, D.A., Energy Dissipation in a Frictional Incomplete Contact with Varying Normal Load, *Int. J. Mech. Sci.*, 2012, vol. 55, pp. 13–21.
8. Putignano, C., Ciavarella, M., and Barber, J.R., Frictional Energy Dissipation in Contact of Nominally Flat Rough Surfaces under Harmonically Varying Loads, *J. Mech. Phys. Solids*, 2011, vol. 59, pp. 2442–2454.
9. Liu, L. and Eriten, M., Frictional Energy Dissipation in Wavy Surfaces, *ASME J. Appl. Mech.*, 2016, vol. 83(12), p. 121001.
10. Johnson, K.L., Surface Interaction between Elastically Loaded Bodies under Tangential Forces, *Proc. R. Soc. Lond. A*, 1955, vol. 230(1183), pp. 531–548.
11. Goodman, L.E. and Brown, C.B., Energy Dissipation in Contact Friction: Constant Normal and Cyclic Tangential Loading, *ASME J. Appl. Mech.*, 1962, vol. 29(1), p. 17.
12. Usta, A.D., Shinde, S., and Eriten, M., Experimental Investigation of Energy Dissipation in Presliding Spherical Contacts under Varying Normal and Tangential Loads, *ASME J. Tribol.*, 2017, vol. 139(6), p. 061402.
13. Griffin, J.H. and Menq, C.-H., Friction Damping of Circular Motion and its Implications to Vibration Control, *ASME J. Vib. Acoust.*, 1991, vol. 113(2), pp. 225–229.
14. Jang, Y.H. and Barber, J.R., Effect of Phase on the Frictional Dissipation in Systems Subjected to Harmonically Varying Loads, *Eur. J. Mech. A. Solids*, 2011, vol. 30(3), pp. 269–274.
15. Popov, V.L. and Heß, M., *Method of Dimensionality Reduction in Contact Mechanics and Friction*, Berlin–Heidelberg: Springer, 2015.
16. Popov, V.L. and Hess, M., *Method of Dimensionality Reduction in Contact Mechanics and Friction: A Users Handbook. I. Axially-Symmetric Contacts*, *Facta Universitat. Mech. Eng.*, 2014, vol. 12(1), pp. 1–14.
17. Popov, V.L., Heß, M., and Willert, E., *Handbook of Contact Mechanics. Exact Solutions of Axisymmetric Contact Problems*, Berlin: Springer, 2019.